

The Transcriptional Landscape of Hematopoietic Stem Cell Ontogeny

Shannon McKinney-Freeman,^{1,2,12} Patrick Cahan,^{1,12} Hu Li,^{3,4,12} Scott A. Lacadie,¹ Hsuan-Ting Huang,¹ Matthew Curran,¹ Sabine Loewer,¹ Olaia Naveiras,¹ Katie L. Kathrein,¹ Martina Konantz,^{5,6} Erin M. Langdon,¹ Claudia Lengerke,⁵ Leonard I. Zon,^{1,7,8,9} James J. Collins,^{3,4,7} and George Q. Daley^{1,7,8,10,11,*}

¹Division of Pediatric Hematology/Oncology, Children's Hospital Boston and Harvard Medical School, Harvard Stem Cell Institute, Boston, MA 02115, USA

²Department of Hematology, St. Jude Children's Research Hospital, Memphis, TN 38105, USA

³Department of Biomedical Engineering, Center for BioDynamics and Center for Advanced Biotechnology, Boston University, Boston, MA 02215, USA

⁴Wyss Institute for Biologically Inspired Engineering, Harvard University, Boston, MA 02115, USA

⁵Division of Hematology and Oncology, University of Tuebingen Medical Center II, 72076 Tuebingen, Germany

⁶Max Planck Institute for Developmental Biology, Department III – Genetics, Spemannstrasse 35, 72076 Tuebingen, Germany

⁷Howard Hughes Medical Institute

⁸Stem Cell Transplantation Program and Children's Hospital Boston, Boston, MA 02115, USA

⁹Dana Farber Cancer Institute, Boston, MA 02115, USA

¹⁰Division of Hematology, Brigham and Women's Hospital, Boston, MA 02115, USA

¹¹Department of Biological Chemistry and Molecular Pharmacology, Harvard Medical School, Broad Institute, Boston, MA 02115, USA

¹²These authors contributed equally to this work

*Correspondence: george.daley@childrens.harvard.edu

<http://dx.doi.org/10.1016/j.stem.2012.07.018>

SUMMARY

Transcriptome analysis of adult hematopoietic stem cells (HSCs) and their progeny has revealed mechanisms of blood differentiation and leukemogenesis, but a similar analysis of HSC development is lacking. Here, we acquired the transcriptomes of developing HSCs purified from >2,500 murine embryos and adult mice. We found that embryonic hematopoietic elements clustered into three distinct transcriptional states characteristic of the definitive yolk sac, HSCs undergoing specification, and definitive HSCs. We applied a network-biology-based analysis to reconstruct the gene regulatory networks of sequential stages of HSC development and functionally validated candidate transcriptional regulators of HSC ontogeny by morpholino-mediated knockdown in zebrafish embryos. Moreover, we found that HSCs from *in vitro* differentiated embryonic stem cells closely resemble definitive HSCs, yet lack a Notch-signaling signature, likely accounting for their defective lymphopoiesis. Our analysis and web resource will enhance efforts to identify regulators of HSC ontogeny and facilitate the engineering of hematopoietic specification.

INTRODUCTION

Hematopoietic stem cells (HSCs) have been extensively analyzed via global transcriptional profiling, which has yielded novel insights into their unique biology (Seita and Weissman,

2010). A recent examination of human HSCs and their progeny revealed both hematopoietic cell-type specific and “reused” transcriptional programs (Novershtern et al., 2011). A similarly comprehensive examination of the transcriptome of embryonic HSCs is absent from the literature, largely due to the practical difficulties of prospectively isolating sufficient quantities of highly purified HSCs and precursors from embryos (Godin and Cumano, 2002). The description of *Sox17* as a disparate regulator of fetal versus adult HSCs indicates that distinct molecular pathways likely govern different stages of HSC development (Kim et al., 2007). A deep understanding of the molecular regulation of HSC ontogeny would inform efforts to expand HSCs *in vitro* and induce HSC generation during pluripotent stem cell (PSC) differentiation, as well as illuminate novel disease-causing genes.

Definitive adult-type HSCs are born in the E10.5 aorta-gonads-mesonephros (AGM), and thereafter migrate to the fetal liver (FL), placenta, and bone marrow (Medvinsky et al., 2011). HSCs apparently emerge from a subset of endothelial cells in the ventral aspect of the dorsal aorta (recently reviewed in detail; Medvinsky et al., 2011). Imaging reveals the dramatic “bending” of hemogenic endothelial cells as they move into the aortic space (Kissa and Herbomel, 2010). Although these emergent cells have not been directly demonstrated to be functional HSCs, the preponderance of evidence indicates that definitive HSCs arise from hemogenic endothelium.

Directed differentiation of PSCs to specific lineages for research and cell therapy is a major goal of stem cell biology. Nearly 2 decades of effort has not yielded robust, definitive HSCs from PSCs (McKinney-Freeman and Daley, 2007). Ectopic expression of the homeotic genes *HoxB4* and *Cdx4* produced cells that reconstituted multilineage hematopoiesis in lethally irradiated primary and secondary mice (Kyba et al., 2002; Wang et al., 2005b). Although this approach generated

hematopoietic progenitors with the cardinal stem cell features of self-renewal and multilineage differentiation, these embryonic-stem-cell-derived HSCs (ESC-HSCs) do not faithfully mimic the function or phenotype of whole bone marrow (WBM)-HSCs (Bonde et al., 2008; McKinney-Freeman et al., 2009; Tabayoyong et al., 2009). Recent data proposing the equivalence of hemogenic endothelium and the hemangioblast that arises during ESC differentiation (Lancrin et al., 2009) suggests that discerning the molecular pathways of hematopoietic ontogeny in vivo will provide a roadmap for differentiating definitive HSCs from PSCs in vitro.

Here, we present the most complete analysis of the transcriptional program of definitive HSC ontogeny to date, gleaned from rigorously characterized hematopoietic stem and progenitor cell (HSPC) populations isolated from over 2,500 murine embryos and adult mice. To illuminate combinatorial control of gene expression, we applied a computational analysis that identifies a gene regulatory network for each critical developmental stage (Faith et al., 2007). We then validated several predicted regulators in HSC ontogeny via morpholino knockdown in zebrafish embryos. We discovered that HSCs exist in only three distinct transcriptional states during ontogeny and that a subset of HSCs from E12.5 FL retain the transcriptional signature of their endothelial precursors. Ultimately, we compared the transcriptional profiles of ESCs, ESC-derived hematopoietic progenitors, and ESC-HSCs to their potential in vivo counterparts, and found that ESC-HSCs most closely resemble definitive HSCs but are defective in essential HSC regulatory pathways, perhaps accounting for their functional deficits. Taken together, our unique data set, available to the stem cell community as a searchable web resource (<http://hsc.hms.harvard.edu>), illuminates aspects of hematopoietic development that will prove valuable for research in developmental hematopoiesis and in vitro directed differentiation.

RESULTS

Acquisition of HSC Gene Expression Profiles throughout Murine Ontogeny

The technical challenges of purifying HSCs to absolute homogeneity from FL and WBM has not precluded the derivation of important biological insights from analysis of the global gene expression profiles of highly purified populations of primitive hematopoietic progenitors (Kiel et al., 2005; Park et al., 2003; Seita and Weissman, 2010). Here, we restricted our purification scheme to surface markers that enrich functionally for hematopoietic repopulation (yolk sac [YS], placenta, FL, WBM, and ESC-HSCs) or HSC precursors (embryoid body [EB]-derived cells and AGM) (Figure 1A and Table 1). E9 YS CD41⁺c-kit⁺ CD34⁺ cells can contribute to life-long hematopoiesis when transplanted into neonates (Ferkowicz et al., 2003). E11.5 AGM HSCs are exceedingly rare (one to three functional HSCs per embryo; Kumaravelu et al., 2002). However, between E11.5 and E12.5, HSCs expand dramatically in the placenta and FL (Kumaravelu et al., 2002; Taoudi et al., 2005, 2008). This expansion results partly from an acceleration in de novo HSC specification from VE-cadherin⁺CD45⁺ AGM hemogenic precursors (Taoudi et al., 2008). To capture the molecular transition from hemogenic endothelium to definitive HSCs, we isolated

VE-cadherin⁺CD45⁺ cells from E11.5 AGM and HSCs from E12.5 placenta and FL. We also collected HSCs from E13.5 FL, E14.5 FL, adult WBM, and ESCs (McKinney-Freeman et al., 2008). Samples were double sorted into lysis buffer via fluorescence-activated cell sorting (FACS) to assure cell purities of >95%, minimal loss of material, and maximal RNA integrity (Figure 1B and Figure S1 available online). Three to six biological replicates were collected for each population. We generated gene expression profiles using Affymetrix gene chips and performed computational analysis as described below.

Embryonic HSCs Exist in Three Predominant Transcriptional States

Pearson correlations between biological replicates revealed that most samples within a group were well correlated (Figure S2A). Hierarchical clustering and principal component analysis (PCA) reveal that embryonic hematopoietic populations segregate into three transcriptionally distinct groups, designated as “YS-like,” “Specifying HSCs,” and “Definitive HSCs” (Figures 2A and 2B). Placenta and AGM samples cluster together (Figures 2A and 2B), confirming recent data that both are sites of hematopoietic specification (Rhodes et al., 2008). Interestingly, two E12.5 FL samples align with the AGM, whereas four align with later-stage FL and WBM HSCs (Figure 2A). We termed the AGM-like E12.5 FL samples “FL12 A,” and the FL-like E12.5 FL samples “FL12 F.” FL12 F, E13.5 FL, E14.5 FL, and WBM-HSCs cluster as one group (i.e. Definitive HSCs) while E9 YS clusters separately with EB-derived hematopoietic progenitors. Definitive HSCs isolated from FL across 2 days of embryonic development (E12.5–14.5) are nearly indistinguishable by gene expression. Nine genes were differentially expressed in FL12 F versus E13.5 FL and only five genes distinguished E13.5 from E14.5 (<http://hsc.hms.harvard.edu>). In contrast, 619 genes were differentially expressed between AGM and FL12 F HSCs (<http://hsc.hms.harvard.edu>). The clustering of FL12 A with placenta/AGM rather than FL/WBM suggests that the transcriptional signature of HSCs immediately upon arrival in the FL represents a critical transitional stage from hemogenic endothelium to definitive HSCs that can be observed fortuitously in some embryos (Figures 2A and 2B). Although AGM and FL12 A cluster together, they are transcriptionally distinct when specific hematopoietic genes are examined (Figure S2B). In total, our data reveal that AGM and FL12 A are distinct, yet transcriptionally related cell populations.

To determine whether differences in the HSPC gene regulatory network (GRN) contribute to the three distinct transcriptional states of developing HSCs, we first identified the context-dependent GRNs of 44 distinct cell types and tissues, including HSPCs, using publicly available data (Supplemental Experimental Procedures). There are three components to each GRN: genes expressed by a cell type or tissue, the transcription factors (TFs) predicted to regulate these genes, and cooperating gene sets that must be highly expressed for the TFs to exert a regulatory influence (contexts). We compared the expression of the HSPC GRN in YS and AGM to WBM (Figure 2C). The expression of the HSPC regulators *Erg*, *Nfe2*, *Hoxa9*, and *Hlf* did not reach an adult HSC expression level in the YS and AGM. Also, *Tulp4*, a predicted repressor of the HSPC GRN, is highly expressed in both the YS-like and Specifying HSCs.

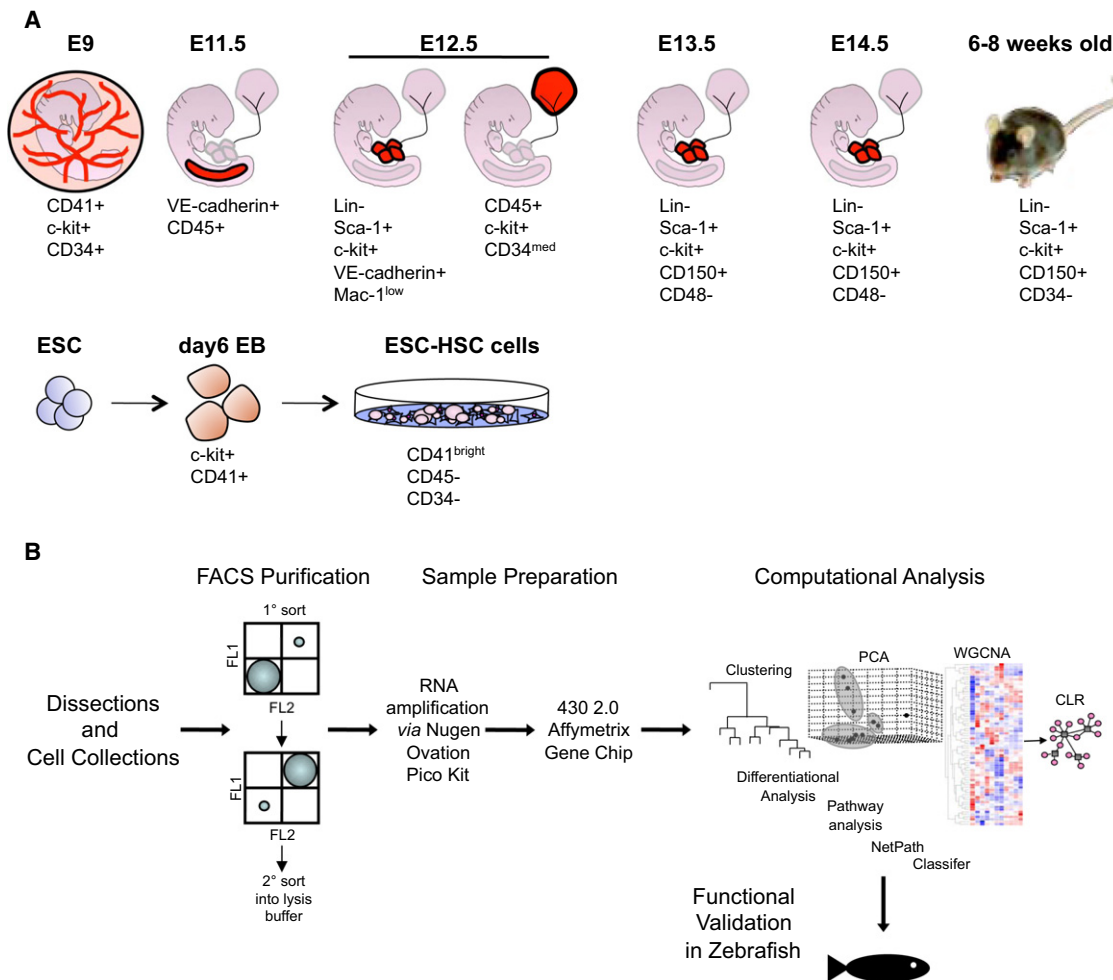


Figure 1. Acquisition of Global Gene Expression Profiles of HSC Compartments throughout Murine Ontogeny

(A) Outline of the developmental time points, embryonic tissues, and ESC-derived populations examined. See also Figure S1.

(B) RNA was collected from double sorted cells, amplified, and then hybridized to 430 2.0 Affymetrix gene chips. The resulting data were analyzed by unsupervised hierarchical clustering, PCA, Naive Bayesian classifier, WGCNA, GRN reconstruction by CLR, differential expression analysis, and GSEA prior to functional studies in zebrafish.

However, *Myb*, *Gata2*, *Tal1*, *Etv6*, *Prdm5*, and *Homez* had low expression only in Specifying HSCs, suggesting that this difference contributes to the distinct states of the YS-like and Specifying groups. Examining the progression of GRN changes in the Definitive HSC population from FL12 to FL14, we found that *Fos* and *Fosb* are downregulated in highly proliferative FL HSCs (Figure 2C), consistent with their role as gatekeepers to HSC mitotic entry (Okada et al., 1999).

Hemogenic Endothelial HSC Precursors Share Transcriptional Overlap with Macrophages

Our data represent the first global expression profiling of HSPCs and their precursors from the AGM, YS, and placenta. To determine the global resemblance of these populations to known, adult cell populations, we applied a Naive Bayesian classifier that calculates the probability that an unknown sample is indistinguishable from known cells types and tissues (Supplemental Experimental Procedures). HSCs from WBM, FL12 F, E13.5 FL, E14.5 FL, E9 YS, E12.5 placenta, E11.5 AGM, day-6 EB-derived

cells, and ESC-HSCs all classified as HSPCs (Figure 3A). Surprisingly, E11.5 AGM hemogenic precursors also scored positively for similarities to macrophages, microglia, and osteoclasts. This likely does not result from contamination because the E11.5 AGM population is uniformly composed of small, blast-like cells that do not resemble macrophages (Taoudi et al., 2005). The set of genes contributing most significantly to the macrophage classification (Figure S3A) is enriched in the Gene Ontology (GO) biological processes of “cell migration,” “blood vessel development,” and “inflammatory response” (corrected $p < 0.01$), suggesting that AGM-derived cells and macrophages utilize common genetic programs to facilitate their migratory behavior and that these cells have remnants of their endothelial origin. The FL12 A samples also classified as macrophages, despite being isolated on the basis of a distinct cell surface phenotype that included the depletion of mature hematopoietic lineages, including macrophages.

We speculated that differential activity of the regulatory network governing the macrophage program might account for

Table 1. Description of Purified HSPCs

Cell Source	Days of Embryonic Development/Differentiation	Total No. Biological Replicates ^c	Total Number of Embryos Dissected	No. Cells/Sample ^e (×1000)	Cell Surface Phenotype of Purified HSPC
Yolk sac	E9 ^a	8	198	23 ± 10.5	CD41 ⁺ CD34 ⁺ c-kit ⁺
AGM	E11.5	10	587	4.1 ± 2.5	VE-cadherin ⁺ CD45 ⁺
Placenta	E12.5	9	485	75.8 ± 55	CD45 ⁺ CD34 ^{med} c-kit ⁺
Fetal liver	E12.5	9	367	3.4 ± 0.9	Lin ⁻ Sca-1 ⁺ c-kit ⁺ VE-cadherin ⁺ Mac-1 ^{low}
Fetal liver	E13.5	6	140	6.5 ± 3.4	Lin ⁻ Sca-1 ⁺ c-kit ⁺ CD150 ⁺ CD48 ⁻
Fetal liver	E14.5	6	458	27.8 ± 11	Lin ⁻ Sca-1 ⁺ c-kit ⁺ CD150 ⁺ CD48 ⁻
WBM	adult	6	276 ^d	90 ± 50	Lin ⁻ Sca-1 ⁺ c-kit ⁺ CD150 ⁺ CD34 ⁻
Embryoid body	day 6	8	—	nr	c-kit ⁺ CD41 ⁺
ESC-HSC	day 10–14 ^b	3	—	1,000 ± 0	CD41 ^{bright} CD45 ⁻ CD34 ⁻
		total	2,511		

nr, not recorded.

^aSomite pairs = 18–22.

^bDay-6 EB-derived cells were expanded on OP9 stroma for 10–14 days after infection with retroviral HoxB4 prior to fractionation via FACS.

^cSum of replicates collected for array and fluidigm analysis.

^dIndicates total number of mice.

^eAccording to cell count of FACSAria after secondary sort into lysis buffer.

the ability of hemogenic endothelial cells to transiently pass through a macrophage-like transcriptional state. To explore this, we again leveraged the context-dependent GRNs of 44 cell types and tissues, comparing the expression of the macrophage GRN in the AGM and FL-derived HSCs to primary macrophages. The expression of most macrophage positive regulators was unchanged (Figure 3B) in the AGM and FL12 A samples. However, *Sfp1*, a master regulator of myeloid and lymphoid differentiation, does not reach the macrophage level of expression (Figure 3B). This is significant because *Sfp1* is autoregulated in differentiated myeloid cells, a mechanism by which cells are able to stabilize transcriptional states (Leddin et al., 2011). These results suggest a model in which nascent HSCs temporarily access a macrophage-related transcriptional program, perhaps to facilitate their migration to the FL. Low *Sfp1* expression may ensure that this state is transient.

ESC-Derived Hematopoietic Progenitors and HSCs Cluster with Distinct In Vivo Populations

EB-derived hematopoietic progenitors express c-kit and CD41 (McKinney-Freeman et al., 2008; Mikkola et al., 2003) and acquire repopulating activity when exposed to ectopic homeobox gene expression and OP9 coculture (Wang et al., 2005a). Moreover, retroviral integration site analysis reveals clonal multilineage lymphoid-myeloid engraftment of primary and secondary animals, thereby reflecting the cardinal features of HSCs—self-renewal and multipotency (Wang et al., 2005a). Although *Cdx-Hox* modified EB cells are the most robust ESC-HSCs reported to date, they fail to fully reconstitute the in vivo lymphoid compartment and display an aberrant cell surface phenotype (McKinney-Freeman et al., 2009). A better understanding of how these ESC-HSCs relate to embryonic HSCs

would inform protocols for deriving HSCs from PSCs or nonhematopoietic tissues via direct conversion. Thus, we compared the gene expression profiles of CD41^{Bright}CD34⁻CD45⁻ ESC-HSCs, c-kit⁺CD41⁺ day-6 EB-derived cells, and ESCs to the developmental data set (Figure 1 and Table 1). ESC-HSCs clustered mostly tightly with FL and WBM HSCs (Figures 2A and 2B) and were distinct from midgestation in vivo populations (i.e. E9 YS) and their cells of origin (i.e. c-kit⁺CD41⁺ EB-derived cells). As anticipated, EB-derived c-kit⁺CD41⁺ cells clustered with E9 YS, reflecting the known similarity of EB-derived and YS hematopoiesis (Keller et al., 1993). Thus, despite their aberrant function, ESC-HSCs are most similar to HSC populations with a definitive, adult-like HSC fate.

Pair-Wise Comparisons

Because the expression of few known HSC regulators fluctuated during HSC ontogeny (Figure S2B), we next assessed differentially expressed genes between each population for enrichment of GO biological processes and canonical signaling pathways (Figures S4A and S4B). Gene Set Enrichment Analysis (GSEA) was applied to pair-wise comparisons between all populations and major biological groups (i.e. YS-like, Definitive, and Specifying HSCs). As expected, ESC were enriched in the GO category “negative regulation of cell differentiation,” and all embryonic populations were enriched in active cell cycle categories (e.g., “cell division,” “cell cycle,” and “mitosis”) relative to WBM-HSCs, consistent with their known quiescence (Wilson et al., 2009). VE-cadherin⁺CD45⁺ AGM-derived cells were enriched for “cell communication,” “NO biosynthetic processes,” and “positive regulation of angiogenesis” (Figure S4A), reflective of their endothelial origin. AGM and placenta were both enriched for “neutrophil chemotaxis” and “chemotaxis,” suggesting

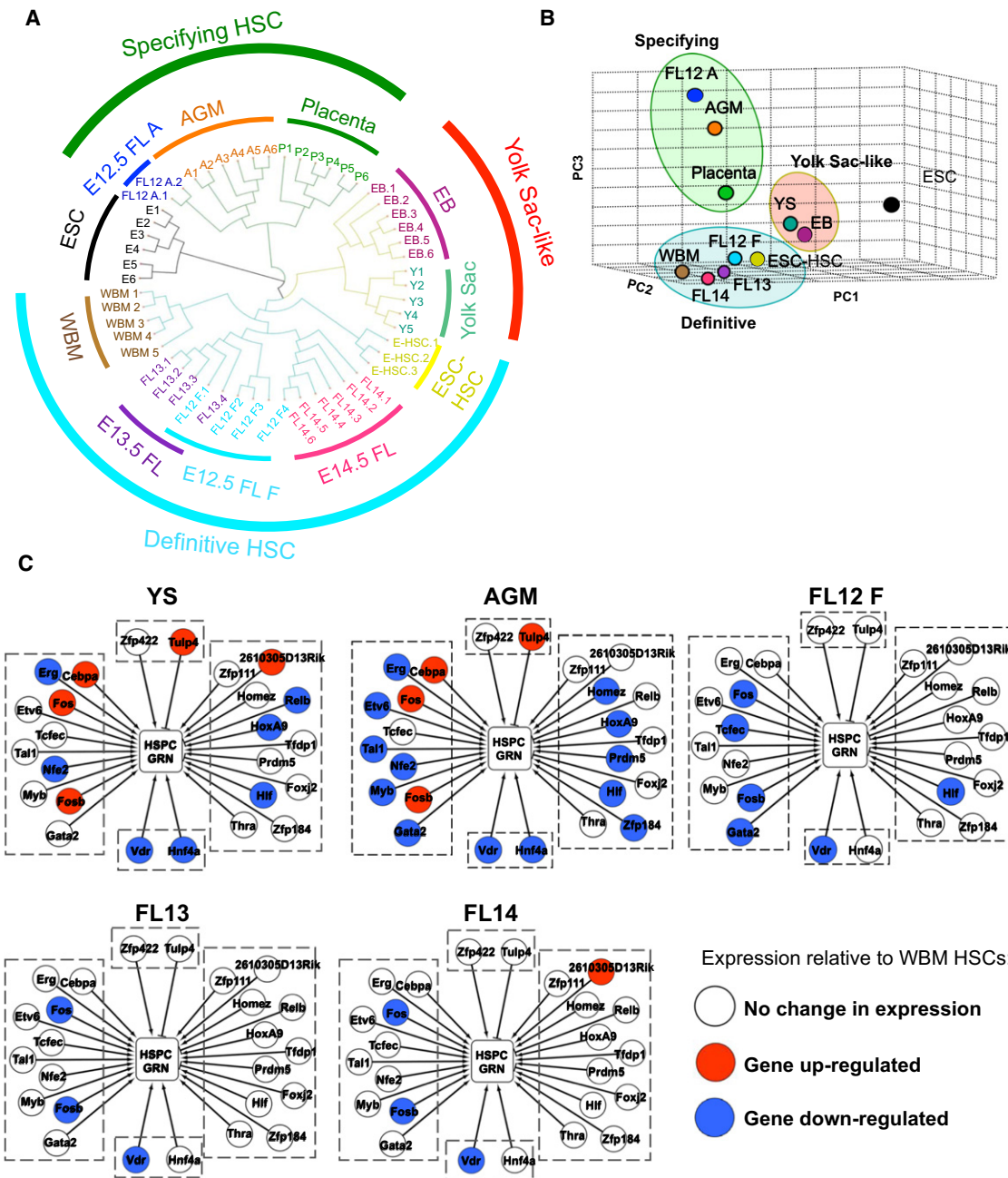


Figure 2. Identification of Distinct Transcriptional and Regulatory Stages of HSC Ontogeny

Results of unsupervised hierarchical clustering (A) and PCA (B). (C) Schematics of the HSPC gene regulatory network (GRN) in YS, AGM, FL12 F, FL13, and FL14 relative to WBM HSCs. This GRN is composed of HSPC expressed genes (center rectangle), transcription factors (TFs) predicted to regulate these genes (circles), and cooperating gene sets that must be highly expressed for the TFs to exert a regulatory influence (contexts, boxed areas). Stimulatory TFs are shown as arrows and inhibitory TFs are shown as blunt lines. Differences in TF expression are shown as red circles (upregulated) or blue circles (downregulated). Only TFs where the absolute value of the log₂ ratio of the given sample versus WBM HSCs exceeds 1 are shown. See also Figure S2.

migratory populations. AGM and placenta are also enriched in “inflammatory response” and “response to lipopolysaccharide” (Figure S4A), consistent with a transcriptional resemblance to macrophages (Figure S4A). Analysis of the major biological groups revealed that Specifying HSCs were enriched in chemotaxis, inflammatory response, positive regulation of nitric oxide, biosynthetic process, cell adhesion, positive regulation of angio-

genesis, and the ERK cascade, again consistent with an endothelial origin (Figure 4A) (Krens et al., 2008; Srinivasan et al., 2009).

Next, we determined whether genes regulated in response to the 20 NetPath signaling pathways (Kandasamy et al., 2010) were enriched in the YS-like, Definitive, and Specifying populations. Each NetPath-annotated signaling pathway has two

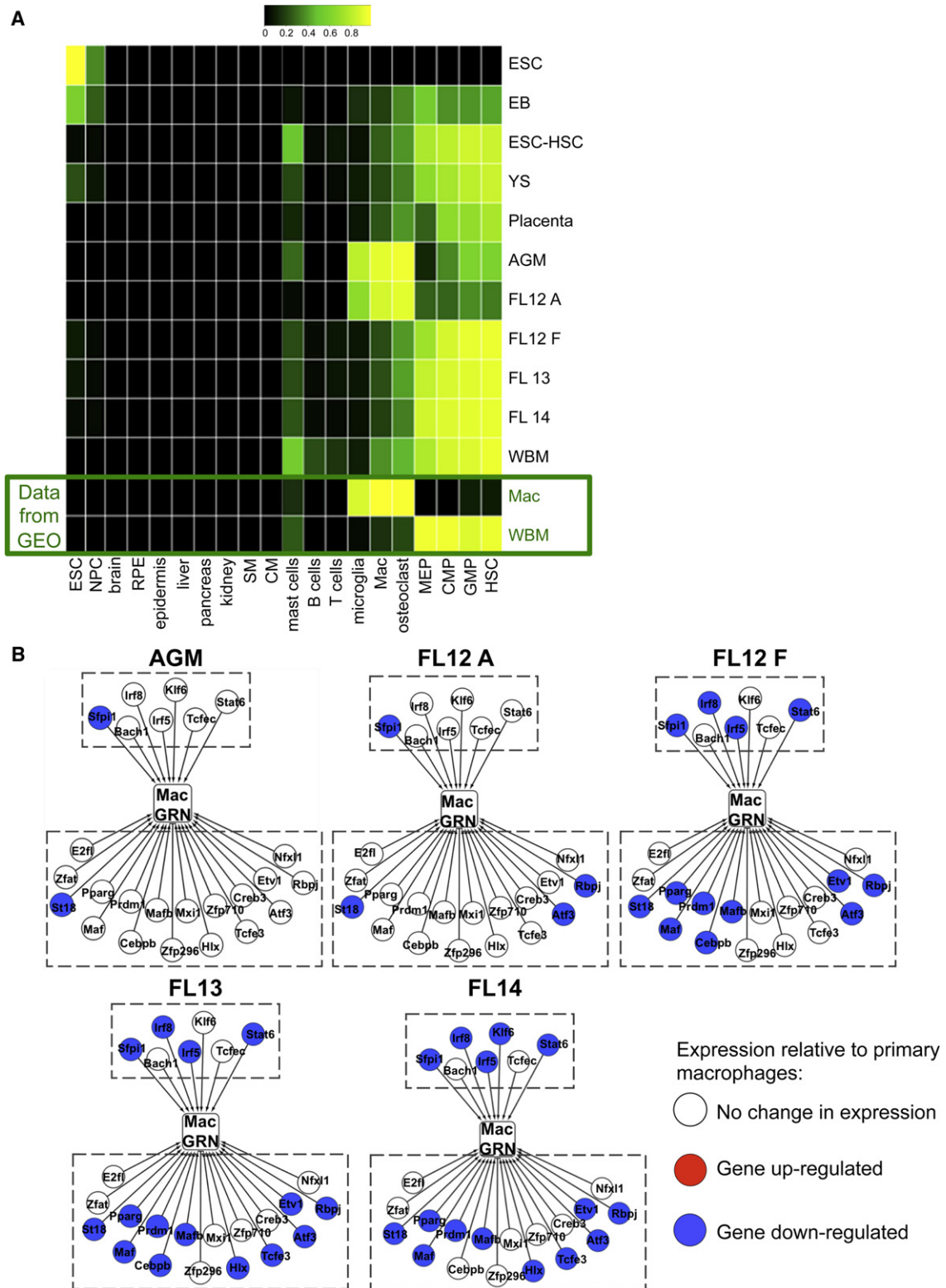


Figure 3. Comparison of HSCs in Ontogeny to Adult Tissues and Cell Types

(A) A Naive Bayesian classifier was used to assess transcriptional overlap with 44 tissues and cell types. The results of 20 of these comparisons are displayed (all other reference tissues and cell types were negative). NPC, neural progenitor cells; RPE, retinal pigment epithelium; SM, skeletal muscle; CM, cardiac muscle; Mac, macrophage; MEP, megakaryocyte-erythrocyte progenitor; CMP, common myeloid progenitor; GMP, granulocyte-monocyte progenitor. Each row is a biological group (i.e. WBM HSCs), and each column is a known tissue or cell type. The classifier determines the posterior probability that a sample is

gene sets: genes upregulated in response to a pathway and genes downregulated. Genes upregulated in response to Wnt and IL-3 signaling were enriched in Specifying HSCs (Figure 4B), in agreement with reports that Wnt and IL-3 signaling promote HSC specification (Goessling et al., 2009; Robin et al., 2006). Notably, *in vivo* Definitive HSCs were enriched in genes targeted by Notch signaling relative to ESC-HSCs (Figure 4B and Figure S4B), suggesting that the aberrant functionality of ESC-HSCs may be due to a lack of specification via Notch signaling.

Identification of Transcriptional Regulators of HSC Ontogeny

To identify coordinately expressed genes, we applied the network-based Weighted Gene Coexpression Network Analysis clustering algorithm (WGCNA) and detected 66 modules ranging in content from 24 to 1,752 genes (Figure 5 and Figure S5A). A complete list of genes assigned to each module is available on the companion website (<http://hsc.hms.harvard.edu>). Because genes within a module are highly positively correlated, we summarized their expression as the median of the standardized expression of each gene within a given module, resulting in a single module value at each developmental time point (Figure 5 and Figure S5A). Twenty-six modules are stage enriched (i.e., more highly expressed in a single stage than all other stages; corrected $p < 0.01$; Figure 5). Thirteen modules were characteristic of Definitive HSCs (highest in FL12 F, FL13, FL14, WBM, ESC-HSCs), eleven for Specifying HSCs (highest in AGM, placenta, FL12 A), and five for YS-like (highest in EB and YS), and ten reflected the *in vitro* state (highest in ESC, EB, and ESC-HSCs; Figure 5).

To identify the GRN active in HSC development, we used the Context Likelihood of Relatedness (CLR) algorithm to identify putative transcriptional regulators (TRs) of each module (Figure S6A) (Faith et al., 2007; Taylor et al., 2008). CLR uses mutual information rather than linear correlation to identify significant relationships between TRs and target genes, and has accurately reconstructed mammalian GRN (Faith et al., 2007; Taylor et al., 2008). We applied CLR to each gene module and 1,623 TRs, computing the mutual information between module profiles and the expression profile of each TR. This analysis identified a GRN consisting of 1,147 putative regulatory relationships (FDR < 0.05) with 0 to 53 (median = 17) regulators per module and 0 to 7 modules per regulator. A table of the complete GRN (TRs and putative target modules) is available on the companion website. For clarity, we show the network consisting of CLR predictions at the 0.01 FDR threshold (Figure S6A). The network is scale free, indicating that a small number of nodes act as hubs with edges to a large number of other nodes, consistent with other network analyses of GRN (Figure S6B) (Barabási and Oltvai, 2004).

To assess the reproducibility of our gene expression data, we analyzed the exemplars and top three predicted regulators of 22 modules via the Fluidigm microfluidic qRT-PCR platform

(Table S1, Figures S5B–S5E). We collected multiple additional independent biological replicates of EB-derived cells, ESC-HSCs, YS, placenta, AGM, E12.5 FL, E13.5 FL, and WBM (Table 1) and compared the microarray intensities of each gene at each stage to qRT-PCR-based delta Cts (normalized to *Rps29*). We saw high concordance between the two platforms ($R^2 = 0.5446$, $p < 4.4 \times 10^{-111}$, Figures S5C and S5D). Figure S5E depicts the results for five Definitive HSC modules, revealing that at the gene level, the Affymetrix expression levels are recapitulated by Fluidigm. In total, 60/80 candidate genes (at a cutoff of $p < 0.10$) were validated by Fluidigm, confirming the fidelity of our data set.

Hypothesizing that highly connected (“hub”) genes are more likely to be important in HSCs, we looked for overlap in the CLR predictions of modules with a Definitive HSC signature (i.e., M7, M10, M11, M12, M23, M26, M35, M37, M42, M50, M8, and M9; Figure 6A). Regulators predicted for more than one of these modules are labeled in Figure 6A. Many of these hub regulators have already been implicated in hematopoiesis, though not necessarily in HSC development, including *HoxA9*, *Vdr*, *Hlf*, *Lmo2*, *Bcl11a*, *Prdm16*, *Gfi1*, and *Mllt3* (Chuiikov et al., 2010; Hirose et al., 2010; Hock et al., 2004; Jeanson and Scadden, 2010; Lawrence et al., 1997; Magnusson et al., 2007; Pina et al., 2008; Sankaran et al., 2008). These results confirm that hub genes may be key regulators of HSC function and/or development.

To functionally determine if our computational predictions were indeed able to identify gene candidates involved in definitive hematopoiesis, Definitive HSC hub genes *Prdm16*, *Mllt3*, *Atf3*, *Msrb2*, and *Rfx5* (Figure 6A), as well as *Gfi1b*, predicted regulator of definitive module M10, and *Tulp4*, a CLR predicted positive regulator of Specifying modules 19 and 28 and negative regulator of Definitive HSC module 7, were selected for knockdown in zebrafish embryos. *Mllt3* is also a Specifying hub gene, predicted to regulate two Specifying modules (M28 and M40). Zebrafish represents a tractable system that faithfully reflects mammalian hematopoiesis and thus allows us to rapidly interrogate a role for these genes in this process *in vivo*. Embryos were injected at the one-cell stage with morpholinos targeting these gene candidates and were assayed at 36 hr postfertilization (hpf) by *in situ* hybridization for *c-myb* and *Runx1*, markers for HSPC/myeloid cells and HSPCs, respectively (Jin et al., 2009).

Mllt3 morphants displayed a significant loss of both *c-myb* and *Runx1* staining in the 36 hpf AGM, suggesting a decrease in HSPCs (Figure 6B). While disruption of *Gfi1b* did not affect *c-myb* or *Runx1* expression in the AGM, an increase of *c-myb*+ cells and a decrease of *Runx1*+ cells was seen in the posterior intermediate cell mass (ICM), where erythroid/myeloid progenitors (EMPs) are known to localize (Figure 6B). These data implicate *Gfi1b* in erythroid/myeloid EMP fate choice by suggesting an increase in EMP-derived myeloid progeny, consistent with *Gfi1*'s known role in lineage choice (Hock and Orkin, 2006; Randrianarison-Huetz et al., 2010). *Atf3* morphants showed an

indistinguishable from each of the tissues or cell types in the reference data set. Higher probabilities are bright yellow and low probabilities are dark green and black.

(B) Schematics of the macrophage GRN in AGM, FL12 A, FL12 F, FL13, and FL14 relative to primary macrophages (see legend to Figure 2C for details). Only TFs where the absolute value of the log₂ ratio of the given sample versus primary macrophages exceeds 2 are shown.

See also Figure S3.

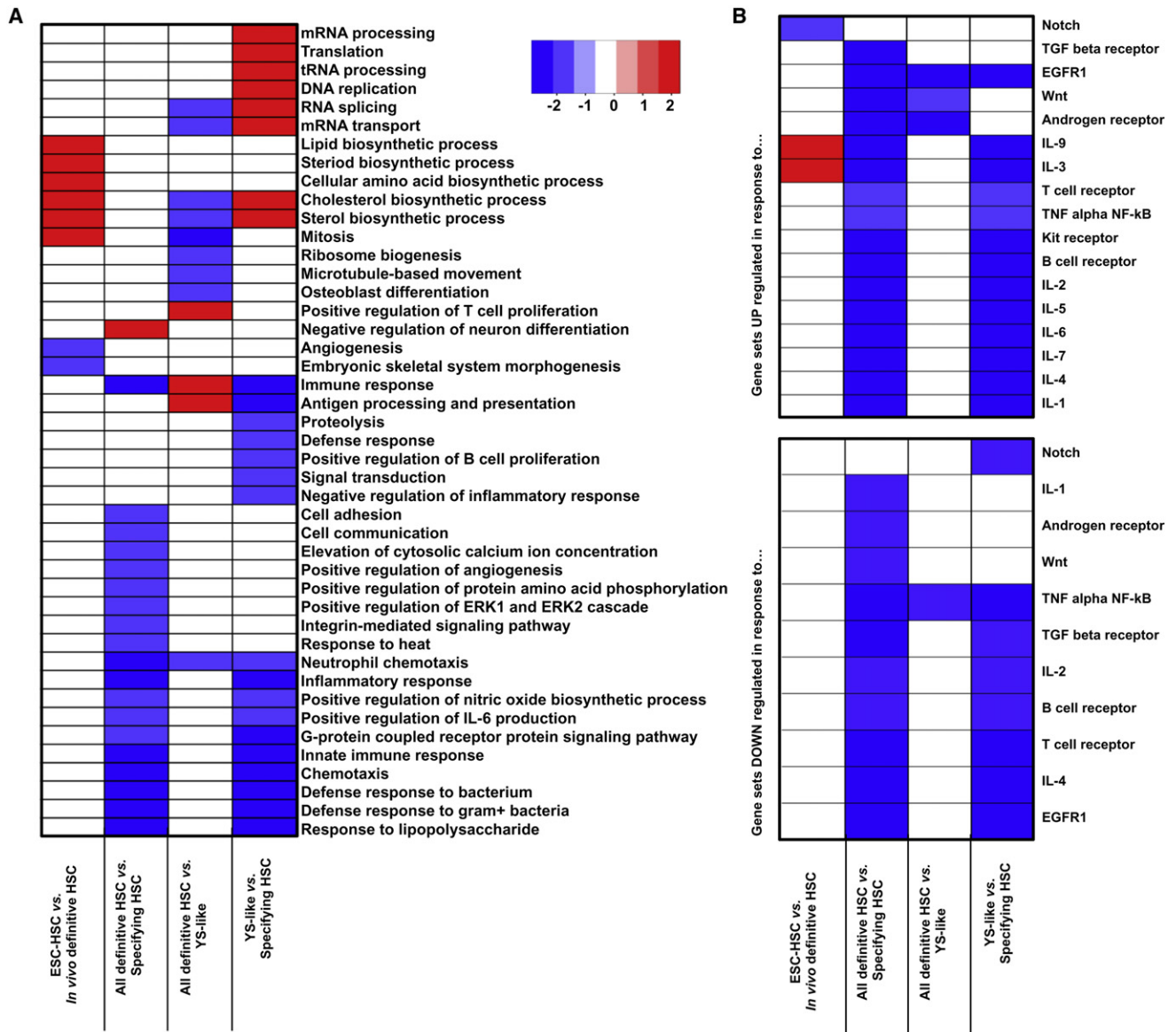


Figure 4. Pathway Enrichment Analysis of Pair-Wise Comparisons between Major Developmental Hematopoietic Groups

(A) GSEA of pair-wise comparisons to find GO biological processes enriched (red) or depleted (blue) between developmental populations.

(B) GSEA of pair-wise comparisons to identify NetPath-annotated signaling pathways transcriptionally activated or suppressed. "In vivo Definitive HSC" includes WBM, FL12 F, E13.5 FL, and E14.5 FL; "Specifying HSC" includes AGM, FL12 A, and placenta; "YS-like" includes EB and YS; and "All definitive HSC" includes ESC-HSCs, WBM, FL12 F, E13.5 FL, and E14.5 FL. Only significant gene sets are shown (Family-wise error rate < 0.05). See also Figure S4.

increase in *Runx1* staining in the AGM with no change in *c-myb* staining (Figure 6B). Likely *Aft3* directly or indirectly regulates *Runx1* transcript levels, given that *Aft3* morphants also displayed no change in *I-plastin* or *CD41*, suggesting that myeloid progeny downstream of HSPCs and HSPC progenitors, respectively, were unchanged (Figures S7B and S7C). *Tulp4* morphants showed a decrease in both *Runx1* and *c-myb* staining in the AGM, suggesting a reduction in HSPCs (Figure 6B). Neither *Aft3* nor *Tulp4* have ever been linked functionally to the regulation of HSCs or hematopoiesis. Thus, our computational data effectively identified these two genes as regulators of HSPC biology.

c-myb expression was clearly reduced in *Prdm16* morphants while *Runx1* expression was maintained (Figure 6B). A loss of *c-myb/Runx1* staining was also observed with a second morpholino targeting a distinct exon of *Prdm16* (Figures S7A and S7D). The development of *c-myb+/Runx1+* cells in the caudal hematopoietic tissue was also impaired in *Prdm16* morphants at 4 days postfertilization (dpf) (Figure 6C). This was not concomitant with an initial loss of proliferation or increase in cell death, as we observed no changes in phospho-histone H3 or apoptosis in *Prdm16* morphants (Figure S7E). Impairment in the formation of *mpo+* and *I-plastin+* myeloid cells and *rag1+* lymphoid cells was also observed at 38 hpf and 4 dpf, respectively (Figures 6D

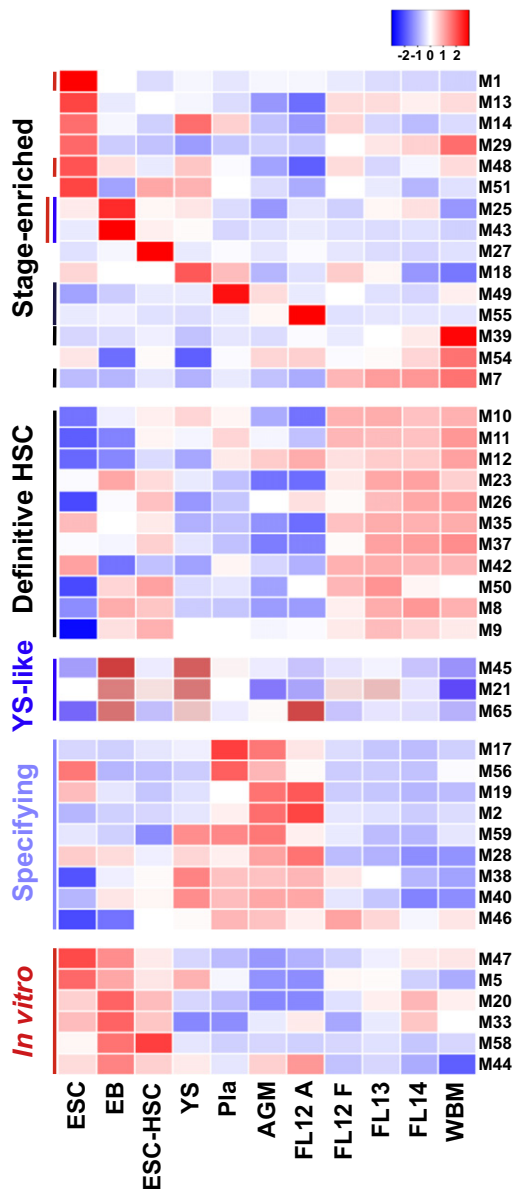


Figure 5. Identification of Stage-Specific Gene Sets

Coregulated gene sets were identified via WGCNA. Sixty-six distinct modules were discovered. A module was considered a Definitive HSC if its expression was significantly higher in definitive HSCs (FL12 F, FL13, FL14, ESC-HSC, and WBM) relative to other samples (Holm-corrected $p < 0.01$). Similarly, modules were annotated as Stage-enriched, Specifying, or In vitro. Each row represents the module profile: a summary of the expression pattern of all genes within a module. See also Figure S5 and Table S1.

and 6E). Notch1 signaling, *ephrinB2* expression, and *flk1* expression were all unperturbed in *Prdm16* morphants, supporting intact hematopoietic and endothelial specification (Figures S7F and S7G). These data suggest proper HSC specification in *Prdm16* morphants, but a failure of HSCP maintenance, and possibly differentiation, as has been suggested by recent mouse studies (Chuiikov et al., 2010; Aguilo et al., 2011). However, a potential defect in HSC migration cannot be excluded by these experiments.

DISCUSSION

Here we present a comprehensive analysis of the transcriptome of developing HSCs from midgestation through adulthood. By application of the network-based WGCNA and CLR algorithms, we identified genes that define discrete stages of HSC development and their putative regulators. Because leukemic transformation often involves the reactivation of developmental genes (e.g., *Lmo2*, *Scl*, *Mll*, and *Runx1*; Ernst et al., 2002; Izraeli, 2004), understanding the transcriptional networks governing HSC development may help unravel mechanisms of hematopoietic malignancy. Further, our data set nominates a host of genes to test for their potential to engineer hematopoietic fates from PSCs, a critical milestone in realizing the clinical potential of patient-specific PSCs.

Our data set complements a recent analysis of the transcriptional circuitry of human postnatal hematopoietic populations by focusing on the transcriptional landscape of embryonic hematopoiesis (Novershtern et al., 2011). *Pbx1* and *Sox4*, identified in our analysis as regulators of Definitive HSC modules M8 and M7, respectively, were also the top-level regulators of the human “HSC-Progenitor” program #865 in this prior study, suggesting conservation of HSC regulators in humans and mice (Novershtern et al., 2011). However, although the HSC-Progenitor program included HOXA9, HOXA10, GATA2, and MEIS1, these genes were split here between modules M7 (*Hox* genes) and M8 (*Gata2* and *Meis1*), suggesting that the establishment of the HSC transcriptional program results from multiple, distinct regulatory programs active during development. Thus, our analysis allowed us to further refine distinct regulatory programs active during HSC ontogeny.

Identification and Functional Validation of Transcriptional Regulators

Computational strategies for inferring mammalian GRNs include modeling expression levels using ordinary differential equations (di Bernardo et al., 2005; Ergün et al., 2007), inferring regulatory relationships based on mutual information between regulators and target genes, and Bayesian network approaches (Faith et al., 2007; Margolin et al., 2006; Segal et al., 2003). As most known hematopoietic regulators in our data set did not dramatically change expression in HSPCs or their precursors during development (Figure S2B), we presumed that the regulators that orchestrate the transitions responsible for each developmental stage remained to be discovered and validated. Thus, we designed a computational strategy to identify stage-specific transcriptional regulators. We applied the CLR algorithm because of its strong performance characteristics and relatively short execution times, which allowed us to iteratively run the algorithm as additional samples were collected and processed (Ciaccio et al., 2010). By extending its application to modules of coordinately expressed genes, we increased CLR’s ability to detect putative target genes (Michoel et al., 2009). This allowed us to discern 66 distinct gene modules and associated TRs. Each module represents an opportunity to develop hypotheses about the regulation of HSC development. Our data is available to the community via a searchable website (<http://hsc.hms.harvard.edu>) that allows users to both explore each WGCNA-generated gene module and its corresponding CLR-predicted

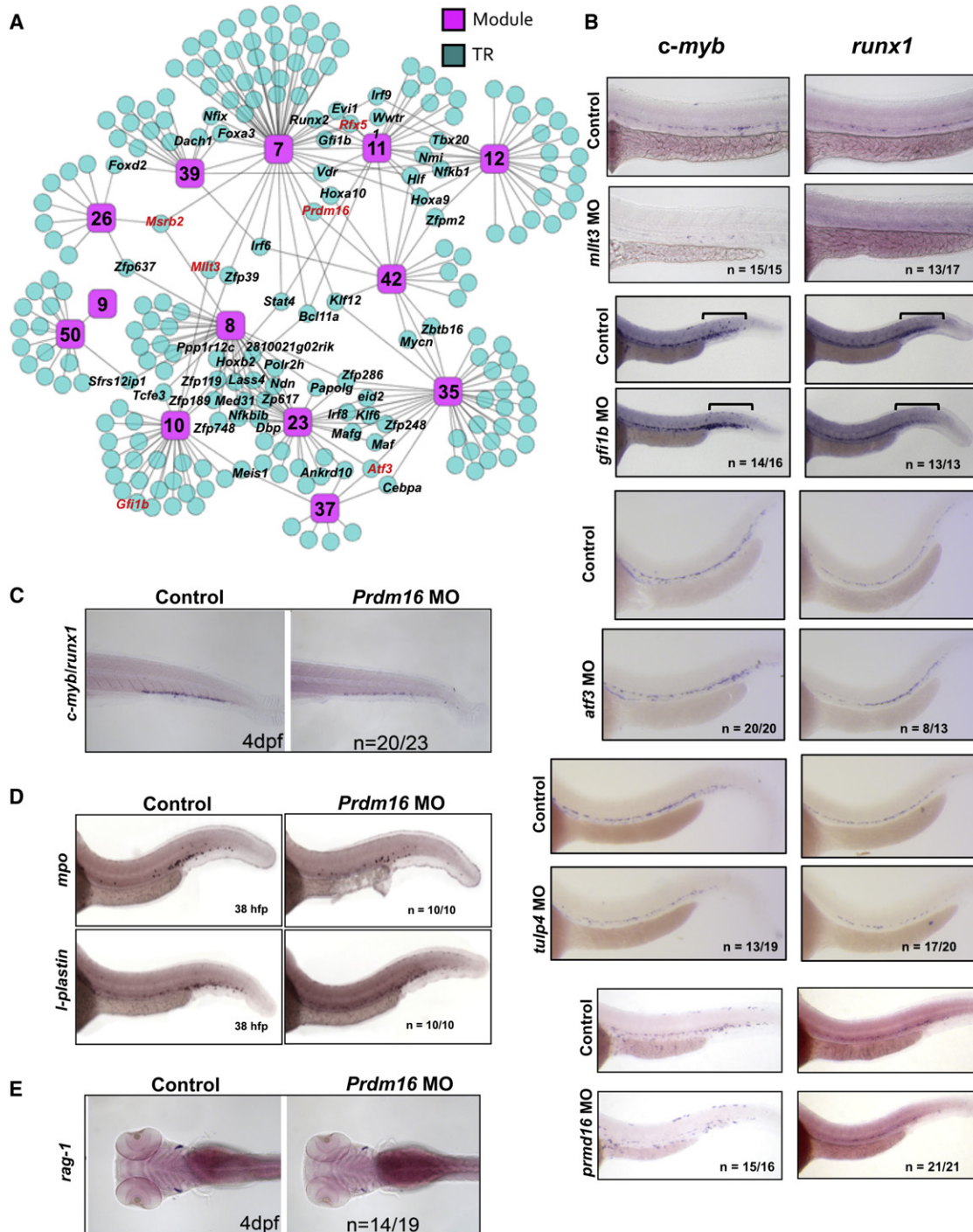


Figure 6. Identification and Validation of Transcriptional Regulators of Discrete Stages of HSC Ontogeny

(A) CLR was applied to identify putative TRs for each module. A network schematic of the CLR-derived predictions at the 0.05 FDR for all Definitive HSC modules is shown. Pink squares represent modules and blue circles represent predicted TRs. “Hub” genes are labeled black. Genes assessed functionally in zebrafish are highlighted in red. A list of all genes predicted to regulate each module can be found at <http://hsc.hms.harvard.edu/>.

(B) Whole-mount in situ hybridization for *c-myb* and *Runx1* was performed at 36 hpf on uninjected embryos or embryos injected with morpholinos (MO) targeting *Mlt3*, *Gfi1*, *Atf3*, *Tulp4*, or *Prdm16*. Bars in *Gfi1b* panels designate the posterior ICM.

(C) The CHT of *Prdm16* morphants was examined 4 dpf for *c-myb/Runx1* expression via whole-mount in situ hybridization.

(D) *Prdm16* morphants were examined via whole-mount in situ hybridization for *mpo* or *l-plastin* expression at 38 hfp.

(E) *Prdm16* morphants were examined via whole-mount in situ hybridization for *rag1* at 4 dpf.

See also Figures S6 and S7.

TRs, and evaluate the expression of genes of interest across the data set.

Our zebrafish studies confirmed a role for *Prdm16*, *Mllt3*, *Gfi1b*, *Aft3*, and *Tulp4*, but not *Rfx5* and *Msrb2* (data not shown), in HSPC biology. These genes were all predicted as HSC regulators by our data set and represent both known and less studied hematopoietic factors. Our data implicate potential roles for both *Mllt3* and *Tulp4* in HSC specification. Importantly, both of these genes are Specifying hub genes: *Mllt3* is a predicted regulator of Specifying modules M40 and M28, and *Tulp4*, of Specifying modules M28 and M19. Although *Mllt3*^{-/-} deficient mice do not have peripheral hematopoietic defects, their HSC compartment is unexplored (Collins et al., 2002; Iida et al., 1993). Preliminary work suggests that ectopic *Mllt3* during murine ESC differentiation enhances the specification of hematopoietic progenitors (data not shown). *Prdm16*, *Gfi1b*, and *Aft3* were each shown to contribute to different aspects of HSC biology, likely downstream of specification: *Gfi1b* was shown to skew the activity of posterior ICM EMPs, consistent with known roles in erythroid/megakaryocyte biology (Hock and Orkin, 2006; Randrianarison-Huetz et al., 2010). Zebrafish *Prdm16* seems required to maintain homeostasis as HSCs differentiate, in agreement with recent data that mice require *Prdm16* for HSC maintenance and function (Aguilo et al., 2011; Chuikov et al., 2010). Although *Aft3* and *Tulp4* were predicted to regulate multiple Specifying and Definitive HSC modules by our analysis, these two genes have never been previously linked to HSC biology. Our finding that morpholino-mediated disruption of these genes in developing zebrafish can perturb the expression of key hematopoietic TRs suggests that these genes may indeed regulate HSC development and/or biology, although further work is needed to clarify their precise roles. Nonetheless, here we showed that multiple genes identified by our computational strategy do indeed have functional consequences on developing hematopoietic populations when disrupted in vivo, establishing that this data set and analysis can identify functionally relevant gene candidates.

Recent reports establishing hemogenic endothelium as the source of definitive HSCs have generated tremendous interest in elucidating the molecular mechanisms governing this transition. *HoxA3*, reported to suppress the hematopoietic signature in endothelium (Iacovino et al., 2011), was identified in our study as a repressor of the specifying module M28 (Figure 5). *Erg*, key for fetal HSCs but dispensable for specification, is negatively correlated with M19, a specifying module, but positively correlated with M10, a definitive HSC module (Figure 5), exactly as one would predict (Taoudi et al., 2011). Thus, our computational analyses successfully identified and classified these known regulators of HSC development.

Embryonic HSCs Can Be YS-like, Specifying, or Definitive

When examined by hierarchical clustering and PCA, the multiple independent HSPC populations interrogated in our study converged on three transcriptionally distinct states: the neonatal repopulating cells of the YS, the nascent HSCs and precursors of the placenta and AGM, and definitive FL and WBM HSCs (Figures 2A and 2B). The relatively few differences within these groups seen by differential expression and GSEA support our

conclusion that there are three states of developing HSC. For example, pathway enrichment analyses revealed only nine and six differentially expressed categories when E13.5 or 14.5 FL HSCs were compared with WBM-HSCs, respectively. Seven of these nine differential groups relate to the already well-described differences in cell cycle status between these groups (Figure S4A). In contrast, 17 and 21 differential groups are seen when the AGM is compared to E13.5 or 14.5 FL HSCs, respectively, suggesting a distinct state. This finding also suggests that the definitive HSC signature is not acquired gradually during gestation, but is specified suddenly around E12.5 as HSCs transition to the FL. This finding highlights again the critical importance of dissecting the molecular regulation of the conversion from a Specifying to a Definitive HSC fate, because this is the most dramatic and critical transition that occurs during HSC ontogeny.

The E12.5 HSC Compartment Is Split between Two Transcriptional States

HSCs, rare in the E10.5–E11.5 conceptus, expand dramatically in the FL and placenta between E11.5 and E12.5 due to an acceleration of de novo HSC specification (Taoudi et al., 2008) (Mikkola et al., 2005). Surprisingly, hierarchical clustering and PCA of our data reveal that the E12.5 HSC compartment is split between an AGM-like transcriptional signature and a WBM-like transcriptional signature: all placenta and FL12 A samples clustered with VE-cadherin⁺CD45⁺ E11.5 AGM while all FL12 F, E13.5 FL, and E14.5 FL samples clustered with WBM HSCs. Thus, some E12.5 HSCs share significant transcriptional overlap with hemogenic endothelial precursors. This could be due to ongoing HSC specification within the early FL or significant numbers of nascent HSC newly arrived from the AGM that have not yet silenced the hemogenic endothelial signature. While VE-cadherin⁺CD45⁺ E11.5 AGM cells express only gamma globin, FL12 A cells express a variety of fetal and adult hemoglobin genes, suggesting a population in transition. Thus, our unique data set and computational analyses suggest a model in which HSCs originating from AGM hemogenic endothelial precursors, and possibly placenta, seed the E12.5 FL and acquire a complete definitive HSC signature over the next few hours of development.

Nascent HSCs Share Transcriptional Overlap with Macrophages and Inflammatory Cells

Although VE-cadherin⁺CD45⁺ AGM-derived and FL12 A cells scored as HSPCs, they also correlated with macrophages via the Naive Bayesian classifier (Figure 3A and Figure S3A). E11.5 AGM-derived VE-cadherin⁺CD45⁺ cells are a mixture of hematopoietic progenitors, adult repopulating cells, and hemogenic precursors that display a uniform blast-like morphology very unlike that of macrophages (Taoudi et al., 2005). Our data suggest that the AGM is enriched for nascent HSPCs that utilize similar molecular mechanisms as macrophages to migrate to the FL. Indeed, analysis of intra-aortic cell clusters by electron microscopy reveals filipodia extensions, suggestive of a population primed to migrate (Medvinsky et al., 1996). VE-cadherin⁺CD45⁺ are likely found in these cell clusters (Taoudi et al., 2005). Like these nascent progenitors, inflammatory cells are programmed to migrate (sites of infection versus FL). Live

imaging recently captured dramatic changes in cell shape and motility as endothelial cells leave the aortic wall and commit to a hematopoietic fate (Kissa and Herbomel, 2010). It is possible that this process employs the same motility pathways as those used by macrophages.

ESC-HSCs Transcriptionally Resemble Definitive HSCs

There have been many unsuccessful attempts to generate PSC-HSCs (McKinney-Freeman and Daley, 2007). Recently, hematopoietic cells have been generated via coculturing human ESCs with AGM-derived stromal lines or reprogramming committed cells directly into hematopoietic progenitors without a pluripotent intermediate, but the degree of hematopoietic engraftment for these engineered populations lags behind accessible human sources like umbilical cord blood (Ledran et al., 2008; Szabo et al., 2010). Although murine ESC-HSCs can robustly engraft lethally irradiated mice (Wang et al., 2005a), they do not faithfully mimic the function or phenotype of WBM-HSCs (McKinney-Freeman et al., 2009). Since ESC-HSCs express high levels of CD41, we hypothesized that they might represent a developmental intermediate. However, our data reveal that ESC-HSCs cluster most closely with FL and WBM-HSCs, rather than E9 YS or day-6 EBs. While it has been thought that *HoxB4* merely expands a hematopoietic progenitor population already specified during EB differentiation, our results suggest that homeotic gene expression, in conjunction with OP9 coculture, serves to respecify a subset of CD41⁺ckit⁺ EB-derived cells toward a definitive HSC fate, as originally argued (Kyba et al., 2002). The aberrant function of ESC-HSCs is likely due to incomplete specification or molecular perturbations caused by constitutive ectopic homeobox gene expression and the absence of critical exogenous and molecular cues. Indeed, *Tek* and *HoxA9* expression is starkly absent from ESC-HSCs relative to FL and WBM HSCs. *Tek* (also known as *Tie2*) regulates HSC maintenance while *HoxA9* is required for normal hematopoiesis (Arai et al., 2004; Lawrence et al., 1997; Takakura et al., 1998). In addition, pair-wise comparison between ESC-HSCs and FL/WBM HSCs revealed the absence of a transcriptional response to Notch signaling, which could explain the inability of these cells to faithfully generate lymphoid cells. Further work is required to determine if rescuing the Notch transcriptional response restores the lymphoid potential of homeobox-derived ESC-HSCs. Most importantly, since ESC-HSCs are closely related to definitive HSCs, yet functionally restricted, they represent a unique opportunity to uncover molecular regulators of definitive HSC function.

EXPERIMENTAL PROCEDURES

Details on embryo dissections, cell culture, zebrafish, Fluidigm validation experiments, and data analysis are described in the [Supplemental Experimental Procedures](#) available online.

Cell Fractionation

Cell sorting was performed as previously described (McKinney-Freeman et al., 2009). For all populations, cells were first collected in PBS and then sorted a second time into lysis buffer (RNAeasy Microkit, QIAGEN).

Microarray

The RNAeasy Microkit (QIAGEN) was used to collect and prepare total RNA for microarray and Fluidigm analysis. The Ovation Picokit (Nugen) was used for

preamplification. Gene expression profiling was performed on Affymetrix 430 2.0 gene chips per standard protocol.

Computational Analysis

Normalization, batch correction, differential analysis, and hierarchical clustering of microarray data are described in detail in the [Supplemental Experimental Procedures](#). WGCNA, a clustering algorithm that selects clustering cutoffs such that the resulting gene network follows a scale-free distribution (Zhang and Horvath, 2005), was used to find sets of positively coregulated genes. Module profiles were computed by calculating the sample median of standardized gene expression values in each module. Module regulatory networks were constructed by applying the CLR algorithm to the matrix consisting of the standardized expression values of 1,171 transcription regulators detected as present in at least one biological group and the module profiles. FDRs were calculated as previously described (Faith et al., 2007). Stage-specific and stage-enriched modules were defined as those expressed higher in one stage versus all other stages (Holm corrected $p < 1 \times 10^{-10}$ and $p < 1 \times 10^{-2}$, respectively). GEO accessions of the mESC samples are GSE16925 and GSE14012. Positive control samples for the classification analysis (Figure 3B) are GSM516564 and GSM463712 for the macrophage and HSC samples, respectively.

ACCESSION NUMBERS

The GEO accession for the newly generated data presented here is GSE37000.

SUPPLEMENTAL INFORMATION

Supplemental Information for this article includes seven figures, one table, and Supplemental Experimental Procedures and can be found with this article online at <http://dx.doi.org/10.1016/j.stem.2012.07.018>.

ACKNOWLEDGMENTS

We thank M.W. Lensch for helpful discussions and critical review of the manuscript, N. Gerry for assistance with gene expression arrays, and J. Daley and S. Lazo-Kallanian of the Dana Farber Cancer Institute (Boston, MA) and Richard Ashman and Jim Houston of St. Jude Children's Research Hospital (Memphis, TN) for expertise in cell sorting and flow cytometry. Fluidigm experiments were performed by the Molecular Genetics Core Facility at Children's Hospital Boston supported by NIH-P50-NS40828 and NIH-P30-HD18655. S.M.F. was supported by NIH grant K01 DK080846. G.Q.D. is supported by grants from the NIH (RO1-DK70055, RO1-DK59279, UO1-HL100001, Progenitor cell biology consortium, R24-DK092760, and special funds from the ARRA stimulus package RC2-HL102815), the Roche Foundation for Anemia Research, Alex's Lemonade Stand, and the Harvard Stem Cell Institute. G.Q.D. is an affiliate member of the Broad Institute, a recipient of Clinical Scientist Awards in Translational Research from the Burroughs Wellcome Fund and the Leukemia and Lymphoma Society, and an investigator of the Manton Center for Orphan Disease Research. P.C. is supported by grants T32HL007623 and 2T32HL66987-11 from the NHLBI. G.Q.D., L.I.Z., and J.J.C. are investigators of the Howard Hughes Medical Institute. L.I.Z. is supported by HHMI and NIH NIDDK 1R24DK092760-01. J.J.C. and H.L. are supported by Howard Hughes Medical Institute, SysCODE (Systems-based Consortium for Organ Design & Engineering), and NIH grant # RL1DE019021, and H.L. is supported by Boston University Clinical and Translational Science Institute (CTS) grant # UL1-TR000157. C.L. was supported by grants from the Deutsche Krebsstiftung (Max Eder Program) and the Deutsche Forschungsgemeinschaft (SFB773). L.I.Z. is a founder and stock holder of Fate, Inc. and a scientific advisor for Stemgent.

Received: July 15, 2011

Revised: February 13, 2012

Accepted: July 23, 2012

Published: November 1, 2012

REFERENCES

- Aguilo, F., Avagyan, S., Labar, A., Sevilla, A., Lee, D.F., Kumar, P., Lemischka, I.R., Zhou, B.Y., and Snoeck, H.W. (2011). Prdm16 is a physiologic regulator of hematopoietic stem cells. *Blood* 117, 5057–5066.
- Arai, F., Hirao, A., Ohmura, M., Sato, H., Matsuoka, S., Takubo, K., Ito, K., Koh, G.Y., and Suda, T. (2004). Tie2/angiopoietin-1 signaling regulates hematopoietic stem cell quiescence in the bone marrow niche. *Cell* 118, 149–161.
- Barabási, A.L., and Oltvai, Z.N. (2004). Network biology: understanding the cell's functional organization. *Nat. Rev. Genet.* 5, 101–113.
- Bonde, S., Chan, K.M., and Zavazava, N. (2008). ES-cell derived hematopoietic cells induce transplantation tolerance. *PLoS ONE* 3, e3212.
- Chaikov, S., Levi, B.P., Smith, M.L., and Morrison, S.J. (2010). Prdm16 promotes stem cell maintenance in multiple tissues, partly by regulating oxidative stress. *Nat. Cell Biol.* 12, 999–1006.
- Ciaccio, M.F., Wagner, J.P., Chuu, C.P., Lauffenburger, D.A., and Jones, R.B. (2010). Systems analysis of EGF receptor signaling dynamics with microwell arrays. *Nat. Methods* 7, 148–155.
- Collins, E.C., Appert, A., Ariza-McNaughton, L., Pannell, R., Yamada, Y., and Rabbitts, T.H. (2002). Mouse Afl9 is a controller of embryo patterning, like Mll, whose human homologue fuses with Afl9 after chromosomal translocation in leukemia. *Mol. Cell. Biol.* 22, 7313–7324.
- di Bernardo, D., Thompson, M.J., Gardner, T.S., Chobot, S.E., Eastwood, E.L., Wojtovich, A.P., Elliott, S.J., Schaus, S.E., and Collins, J.J. (2005). Chemogenomic profiling on a genome-wide scale using reverse-engineered gene networks. *Nat. Biotechnol.* 23, 377–383.
- Ergün, A., Lawrence, C.A., Kohanski, M.A., Brennan, T.A., and Collins, J.J. (2007). A network biology approach to prostate cancer. *Mol. Syst. Biol.* 3, 82.
- Ernst, P., Wang, J., and Korsmeyer, S.J. (2002). The role of MLL in hematopoiesis and leukemia. *Curr. Opin. Hematol.* 9, 282–287.
- Faith, J.J., Hayete, B., Thaden, J.T., Mogno, I., Wierzbowski, J., Cottarel, G., Kasif, S., Collins, J.J., and Gardner, T.S. (2007). Large-scale mapping and validation of *Escherichia coli* transcriptional regulation from a compendium of expression profiles. *PLoS Biol.* 5, e8.
- Ferkowicz, M.J., Starr, M., Xie, X., Li, W., Johnson, S.A., Shelley, W.C., Morrison, P.R., and Yoder, M.C. (2003). CD41 expression defines the onset of primitive and definitive hematopoiesis in the murine embryo. *Development* 130, 4393–4403.
- Godin, I., and Cumano, A. (2002). The hare and the tortoise: an embryonic haematopoietic race. *Nat. Rev. Immunol.* 2, 593–604.
- Goessling, W., North, T.E., Loewer, S., Lord, A.M., Lee, S., Stoick-Cooper, C.L., Weidinger, G., Puder, M., Daley, G.Q., Moon, R.T., and Zon, L.I. (2009). Genetic interaction of PGE2 and Wnt signaling regulates developmental specification of stem cells and regeneration. *Cell* 136, 1136–1147.
- Hirose, K., Inukai, T., Kikuchi, J., Furukawa, Y., Ikawa, T., Kawamoto, H., Oram, S.H., Göttgens, B., Kiyokawa, N., Miyagawa, Y., et al. (2010). Aberrant induction of LMO2 by the E2A-HLF chimeric transcription factor and its implication in leukemogenesis of B-precursor ALL with t(17;19). *Blood* 116, 962–970.
- Hock, H., and Orkin, S.H. (2006). Zinc-finger transcription factor Gfi-1: versatile regulator of lymphocytes, neutrophils and hematopoietic stem cells. *Curr. Opin. Hematol.* 13, 1–6.
- Hock, H., Hamblen, M.J., Rooke, H.M., Schindler, J.W., Saleque, S., Fujiwara, Y., and Orkin, S.H. (2004). Gfi-1 restricts proliferation and preserves functional integrity of haematopoietic stem cells. *Nature* 431, 1002–1007.
- Iacovino, M., Chong, D., Szatmari, I., Hartweck, L., Rux, D., Caprioli, A., Cleaver, O., and Kyba, M. (2011). HoxA3 is an apical regulator of haemogenic endothelium. *Nat. Cell Biol.* 13, 72–78.
- Iida, S., Seto, M., Yamamoto, K., Komatsu, H., Tojo, A., Asano, S., Kamada, N., Ariyoshi, Y., Takahashi, T., and Ueda, R. (1993). MLLT3 gene on 9p22 involved in t(9;11) leukemia encodes a serine/proline rich protein homologous to MLLT1 on 19p13. *Oncogene* 8, 3085–3092.
- Izraeli, S. (2004). Leukaemia — a developmental perspective. *Br. J. Haematol.* 126, 3–10.
- Jeanson, N.T., and Scadden, D.T. (2010). Vitamin D receptor deletion leads to increased hematopoietic stem and progenitor cells residing in the spleen. *Blood* 116, 4126–4129.
- Jin, H., Sood, R., Xu, J., Zhen, F., English, M.A., Liu, P.P., and Wen, Z. (2009). Definitive hematopoietic stem/progenitor cells manifest distinct differentiation output in the zebrafish VDA and PBI. *Development* 136, 647–654.
- Kandasamy, K., Mohan, S.S., Raju, R., Keerthikumar, S., Kumar, G.S., Venugopal, A.K., Telikicherla, D., Navarro, J.D., Mathivanan, S., Pecquet, C., et al. (2010). NetPath: a public resource of curated signal transduction pathways. *Genome Biol.* 11, R3.
- Keller, G., Kennedy, M., Papayannopoulou, T., and Wiles, M.V. (1993). Hematopoietic commitment during embryonic stem cell differentiation in culture. *Mol. Cell. Biol.* 13, 473–486.
- Kiel, M.J., Yilmaz, O.H., Iwashita, T., Yilmaz, O.H., Terhorst, C., and Morrison, S.J. (2005). SLAM family receptors distinguish hematopoietic stem and progenitor cells and reveal endothelial niches for stem cells. *Cell* 121, 1109–1121.
- Kim, I., Saunders, T.L., and Morrison, S.J. (2007). Sox17 dependence distinguishes the transcriptional regulation of fetal from adult hematopoietic stem cells. *Cell* 130, 470–483.
- Kissa, K., and Herbomel, P. (2010). Blood stem cells emerge from aortic endothelium by a novel type of cell transition. *Nature* 464, 112–115.
- Krens, S.F., Corredor-Adámez, M., He, S., Snaar-Jagalska, B.E., and Spink, H.P. (2008). ERK1 and ERK2 MAPK are key regulators of distinct gene sets in zebrafish embryogenesis. *BMC Genomics* 9, 196.
- Kumaravelu, P., Hook, L., Morrison, A.M., Ure, J., Zhao, S., Zuyev, S., Ansell, J., and Medvinsky, A. (2002). Quantitative developmental anatomy of definitive haematopoietic stem cells/long-term repopulating units (HSC/RUS): role of the aorta-gonad-mesonephros (AGM) region and the yolk sac in colonisation of the mouse embryonic liver. *Development* 129, 4891–4899.
- Kyba, M., Perlingeiro, R.C., and Daley, G.Q. (2002). HoxB4 confers definitive lymphoid-myeloid engraftment potential on embryonic stem cell and yolk sac hematopoietic progenitors. *Cell* 109, 29–37.
- Lancrin, C., Sroczyńska, P., Stephenson, C., Allen, T., Kouskoff, V., and Lacaud, G. (2009). The haemangioblast generates haematopoietic cells through a haemogenic endothelium stage. *Nature* 457, 892–895.
- Lawrence, H.J., Helgason, C.D., Sauvageau, G., Fong, S., Izon, D.J., Humphries, R.K., and Largman, C. (1997). Mice bearing a targeted interruption of the homeobox gene HOXA9 have defects in myeloid, erythroid, and lymphoid hematopoiesis. *Blood* 89, 1922–1930.
- Leddin, M., Perrod, C., Hoogenkamp, M., Ghani, S., Assi, S., Heinz, S., Wilson, N.K., Follows, G., Schönheit, J., Vockentanz, L., et al. (2011). Two distinct auto-regulatory loops operate at the PU.1 locus in B cells and myeloid cells. *Blood* 117, 2827–2838.
- Ledran, M.H., Krassowska, A., Armstrong, L., Dimmick, I., Renström, J., Lang, R., Yung, S., Santibanez-Coref, M., Dzierzak, E., Stojkovic, M., et al. (2008). Efficient hematopoietic differentiation of human embryonic stem cells on stromal cells derived from hematopoietic niches. *Cell Stem Cell* 3, 85–98.
- Magnusson, M., Brun, A.C., Lawrence, H.J., and Karlsson, S. (2007). Hoxa9/hoxb3/hoxb4 compound null mice display severe hematopoietic defects. *Exp. Hematol.* 35, 1421–1428.
- Margolin, A.A., Nemenman, I., Basso, K., Wiggins, C., Stolovitzky, G., Dalla Favera, R., and Califano, A. (2006). ARACNE: an algorithm for the reconstruction of gene regulatory networks in a mammalian cellular context. *BMC Bioinformatics* 7 (Suppl 1), S7.
- McKinney-Freeman, S.L., and Daley, G.Q. (2007). Towards hematopoietic reconstitution from embryonic stem cells: a sanguine future. *Curr. Opin. Hematol.* 14, 343–347.
- McKinney-Freeman, S.L., Lengerke, C., Jang, I.H., Schmitt, S., Wang, Y., Philias, M., Shea, J., and Daley, G.Q. (2008). Modulation of murine embryonic stem cell-derived CD41+c-kit+ hematopoietic progenitors by ectopic expression of Cdx genes. *Blood* 111, 4944–4953.
- McKinney-Freeman, S.L., Naveiras, O., Yates, F., Loewer, S., Philias, M., Curran, M., Park, P.J., and Daley, G.Q. (2009). Surface antigen phenotypes

- of hematopoietic stem cells from embryos and murine embryonic stem cells. *Blood* 114, 268–278.
- Medvinsky, A.L., Gan, O.I., Semenova, M.L., and Samoylina, N.L. (1996). Development of day-8 colony-forming unit-spleen hematopoietic progenitors during early murine embryogenesis: spatial and temporal mapping. *Blood* 87, 557–566.
- Medvinsky, A., Rytsov, S., and Taoudi, S. (2011). Embryonic origin of the adult hematopoietic system: advances and questions. *Development* 138, 1017–1031.
- Michoel, T., De Smet, R., Joshi, A., Van de Peer, Y., and Marchal, K. (2009). Comparative analysis of module-based versus direct methods for reverse-engineering transcriptional regulatory networks. *BMC Syst. Biol.* 3, 49.
- Mikkola, H.K., Fujiwara, Y., Schlaeger, T.M., Traver, D., and Orkin, S.H. (2003). Expression of CD41 marks the initiation of definitive hematopoiesis in the mouse embryo. *Blood* 101, 508–516.
- Mikkola, H.K., Gekas, C., Orkin, S.H., and Dieterlen-Lievre, F. (2005). Placenta as a site for hematopoietic stem cell development. *Exp. Hematol.* 33, 1048–1054.
- Novershtern, N., Subramanian, A., Lawton, L.N., Mak, R.H., Haining, W.N., McConkey, M.E., Habib, N., Yosef, N., Chang, C.Y., Shay, T., et al. (2011). Densely interconnected transcriptional circuits control cell states in human hematopoiesis. *Cell* 144, 296–309.
- Okada, S., Fukuda, T., Inada, K., and Tokuhisa, T. (1999). Prolonged expression of c-fos suppresses cell cycle entry of dormant hematopoietic stem cells. *Blood* 93, 816–825.
- Park, I.K., Qian, D., Kiel, M., Becker, M.W., Pihalja, M., Weissman, I.L., Morrison, S.J., and Clarke, M.F. (2003). Bmi-1 is required for maintenance of adult self-renewing haematopoietic stem cells. *Nature* 423, 302–305.
- Pina, C., May, G., Soneji, S., Hong, D., and Enver, T. (2008). MLLT3 regulates early human erythroid and megakaryocytic cell fate. *Cell Stem Cell* 2, 264–273.
- Randrianarison-Huetz, V., Laurent, B., Bardet, V., Blobbe, G.C., Huetz, F., and Duménil, D. (2010). Gfi-1B controls human erythroid and megakaryocytic differentiation by regulating TGF-beta signaling at the bipotent erythro-megakaryocytic progenitor stage. *Blood* 115, 2784–2795.
- Rhodes, K.E., Gekas, C., Wang, Y., Lux, C.T., Francis, C.S., Chan, D.N., Conway, S., Orkin, S.H., Yoder, M.C., and Mikkola, H.K. (2008). The emergence of hematopoietic stem cells is initiated in the placental vasculature in the absence of circulation. *Cell Stem Cell* 2, 252–263.
- Robin, C., Ottersbach, K., Durand, C., Peeters, M., Vanes, L., Tybulewicz, V., and Dzierzak, E. (2006). An unexpected role for IL-3 in the embryonic development of hematopoietic stem cells. *Dev. Cell* 11, 171–180.
- Sankaran, V.G., Menne, T.F., Xu, J., Akie, T.E., Lettre, G., Van Handel, B., Mikkola, H.K., Hirschhorn, J.N., Cantor, A.B., and Orkin, S.H. (2008). Human fetal hemoglobin expression is regulated by the developmental stage-specific repressor BCL11A. *Science* 322, 1839–1842.
- Segal, E., Shapira, M., Regev, A., Pe'er, D., Botstein, D., Koller, D., and Friedman, N. (2003). Module networks: identifying regulatory modules and their condition-specific regulators from gene expression data. *Nat. Genet.* 34, 166–176.
- Seita, J., and Weissman, I.L. (2010). Hematopoietic stem cell: self-renewal versus differentiation. *Wiley Interdiscip. Rev. Syst. Biol. Med.* 2, 640–653.
- Srinivasan, R., Zabuawala, T., Huang, H., Zhang, J., Gulati, P., Fernandez, S., Karlo, J.C., Landreth, G.E., Leone, G., and Ostrowski, M.C. (2009). Erk1 and Erk2 regulate endothelial cell proliferation and migration during mouse embryonic angiogenesis. *PLoS ONE* 4, e8283.
- Szabo, E., Rampalli, S., Risueño, R.M., Schnerch, A., Mitchell, R., Fiebig-Comyn, A., Levadoux-Martin, M., and Bhatia, M. (2010). Direct conversion of human fibroblasts to multilineage blood progenitors. *Nature* 468, 521–526.
- Tabayoyong, W.B., Salas, J.G., Bonde, S., and Zavazava, N. (2009). HOXB4-transduced embryonic stem cell-derived Lin-c-kit+ and Lin-Sca-1+ hematopoietic progenitors express H60 and are targeted by NK cells. *J. Immunol.* 183, 5449–5457.
- Takakura, N., Huang, X.L., Naruse, T., Hamaguchi, I., Dumont, D.J., Yancopoulos, G.D., and Suda, T. (1998). Critical role of the TIE2 endothelial cell receptor in the development of definitive hematopoiesis. *Immunity* 9, 677–686.
- Taoudi, S., Morrison, A.M., Inoue, H., Gribi, R., Ure, J., and Medvinsky, A. (2005). Progressive divergence of definitive haematopoietic stem cells from the endothelial compartment does not depend on contact with the foetal liver. *Development* 132, 4179–4191.
- Taoudi, S., Gonneau, C., Moore, K., Sheridan, J.M., Blackburn, C.C., Taylor, E., and Medvinsky, A. (2008). Extensive hematopoietic stem cell generation in the AGM region via maturation of VE-cadherin+CD45+ pre-definitive HSCs. *Cell Stem Cell* 3, 99–108.
- Taoudi, S., Bee, T., Hilton, A., Knezevic, K., Scott, J., Willson, T.A., Collin, C., Thomas, T., Voss, A.K., Kile, B.T., et al. (2011). ERG dependence distinguishes developmental control of hematopoietic stem cell maintenance from hematopoietic specification. *Genes Dev.* 25, 251–262.
- Taylor, R.C., Acquah-Mensah, G., Singhal, M., Malhotra, D., and Biswal, S. (2008). Network inference algorithms elucidate Nrf2 regulation of mouse lung oxidative stress. *PLoS Comput. Biol.* 4, e1000166.
- Wang, L., Menendez, P., Shojaei, F., Li, L., Mazurier, F., Dick, J.E., Cerdan, C., Levac, K., and Bhatia, M. (2005a). Generation of hematopoietic repopulating cells from human embryonic stem cells independent of ectopic HOXB4 expression. *J. Exp. Med.* 201, 1603–1614.
- Wang, Y., Yates, F., Naveiras, O., Ernst, P., and Daley, G.Q. (2005b). Embryonic stem cell-derived hematopoietic stem cells. *Proc. Natl. Acad. Sci. USA* 102, 19081–19086.
- Wilson, A., Laurenti, E., and Trumpp, A. (2009). Balancing dormant and self-renewing hematopoietic stem cells. *Curr. Opin. Genet. Dev.* 19, 461–468.
- Zhang, B., and Horvath, S. (2005). A general framework for weighted gene co-expression network analysis. *Stat. Appl. Genet. Mol. Biol.* 4, 1128.